High temperature stability of anatase films prepared by MOCVD

Materials Transactions, Vol. 49, No. 9 (2008) pp. 2040 to 2046

High Temperature Stability of Anatase Films Prepared by MOCVD

Rong Tu and Takashi Goto

Institute for Materials Research, Tohoku University, Sendai 980-8577, Japan

Highly thermally stable anatase films were prepared by metal-organic chemical vapor deposition (MOCVD) using $Ti(O\text{-}i\text{-}Pr)_2(dpm)_2$ as precursor. The effect of heat treatment on the microstructure, transmittance, optical band gap and refractive index of anatase films was investigated. Anatase films in a single phase were obtained at T_{sub} (substrate temperature) < 723 K. By heat-treating the anatase film at 1273 K, no phase transformation was observed without changing the transmittance and optical band gap, whereas the refractive index increased. A small amount of rutile phase was identified in the anatase film by heat-treating at 1323 K. The anatase films transformed into rutile in a single phase by heat-treating at 1373 K, resulting in a decrease in transmittance and optical bandgap and an increase in refractive index.
[doi:10.2320/matertrans.MRA2008114]

(Received April 3, 2008; Accepted June 4, 2008; Published July 16, 2008)

Keywords: *metal-organic chemical vapor deposition (CVD), phase transition, anatase, rutile*

1. Introduction

Among the polymorphisms of titanium oxide (TiO_2), i.e., anatase, rutile and brookite, the anatase phase has excellent photocatalytic[1] and self-cleaning activities.[2] The anatase would generally transform into rutile around 1000 K resulting in a decrease of photocatalysis.[3] Therefore, it is advantageous to prepare thermally stable anatase hardly transforming to rutile.

Anatase films have been commonly prepared by sol-gel,[4] sputtering,[5] evaporation[6] and CVD.[7,8] It is known that the transformation temperature from anatase to rutile (T_{AR}) would strongly depend on the preparation processing and their conditions.[9] An anatase film prepared by sol-gel transformed into rutile at 1000 K,[10,11] and that prepared by sputtering transformed at 1123 K.[12] On the other hand, the T_{AR} of anatase films and particles prepared by MOCVD are generally higher than those by sol-gel and sputtering. The anatase particles synthesized by CVD using titanium tetrabutoxide (TTB) slightly transformed into rutile between 1073 and 1173 K[13,14] whereas those prepared by using titanium tetraisopropoxide (TTIP) transformed at 1173 to 1273 K.[7] It is known that the T_{AR} may depend on impurity, typically carbon, in the anatase particles,[15] and therefore, it is critical to choose appropriate deposition conditions and a precursor to obtain anatase film with high T_{AR}. In the present study, we have used $Ti(O\text{-}i\text{-}Pr)_2(dpm)_2$ and studied the effect of deposition conditions on the crystal phase and microstructure of TiO_2 films, and then investigated the phase transformation behavior from anatase to rutile.

2. Experimental

A vertical cold-wall type CVD reactor was used to prepare TiO_2 film.[16] A source precursor of $Ti(O\text{-}i\text{-}Pr)_2(dpm)_2$ (bis-dipivaloylmethanato diisopropoxy titanium, $Ti(OCH(CH_3)_2)_2(O_2C_3H(C_4H_9)_2)_2$) was vaporized at 423 K, and carried with Ar gas into the CVD reactor. O_2 gas was separately introduced by using a double tube nozzle, and mixed with the precursor vapor in a mixing chamber placed above a substrate holder. Fused quartz glass plates (10 by 15 by 1 mm) were used as substrates. The total pressure in the CVD reactor (P_{tot}) was controlled between 0.6 to 1.0 kPa. The substrate temperature (T_{sub}) was changed from 573 to 1173 K. The preparation conditions were summarized in Table 1. The anatase films were heat-treated at 1073 to 1373 K in air for 10.8 ks. The crystal structure was studied by X-ray diffraction (XRD). The microstructure and thickness of films were examined by scanning electron microscopy (SEM) and transmission electron microscopy (TEM). The transmittance was measured by a UV-VIS-NIR scanning spectrophotometer (Shimazu UV-3101PC) in the range of 200 to 2000 nm. The refractive index was measured by an ellipsometer (Gartner L116BLC-310) at a fixed wavelength of 632.8 nm.

Table 1 Deposition conditions of TiO_2 film by MOCVD.

Evaporation temperature of precursor, T_{Ti}/K:	423
Substrate temperature, T_{sub}/K:	573–1173
Total pressure in chamber, P_{tot}/kPa:	0.6–1.0
Deposition time, t_{dep}/ks:	0.9
Flow rate of oxygen, $FR_{O_2}/10^{-7}$ m^3 s^{-1}:	16.67
Flow rate of Argon, $FR_{Ar}/10^{-7}$ m^3 s^{-1}:	16.67
Flow rate of total gas, $FR_{tot}/10^{-7}$ m^3 s^{-1}:	33.33

3. Results and Discussion

Figure 1 depicts the X-ray diffraction patterns of TiO_2 films deposited at $P_{tot} = 0.8$ kPa and $T_{sub} = 723$ to 1073 K. At $T_{sub} = 723$ K, anatase TiO_2 films in a single phase with (004) orientation were obtained (Fig. 1(a)). At $T_{sub} = 873$ K, rutile TiO_2 films were obtained in a single phase with (200) orientation (Fig. 1(b)). At $T_{sub} = 1073$ K, mixtures of non-oriented rutile and anatase films were obtained (Fig. 1(c)). Generally, the preferred orientation of film in CVD would be related with the mobility of atoms and the surface energy of crystal plane, and could be explained as follows. The mobility of atoms is low at low T_{sub}, and then the crystal plane with relatively low atom-packing density might form easily. On the other hand, if the atoms have high mobility at high T_{sub}, they can move to a stable site. Thus, the crystal plane with the lowest surface energy would be preferentially

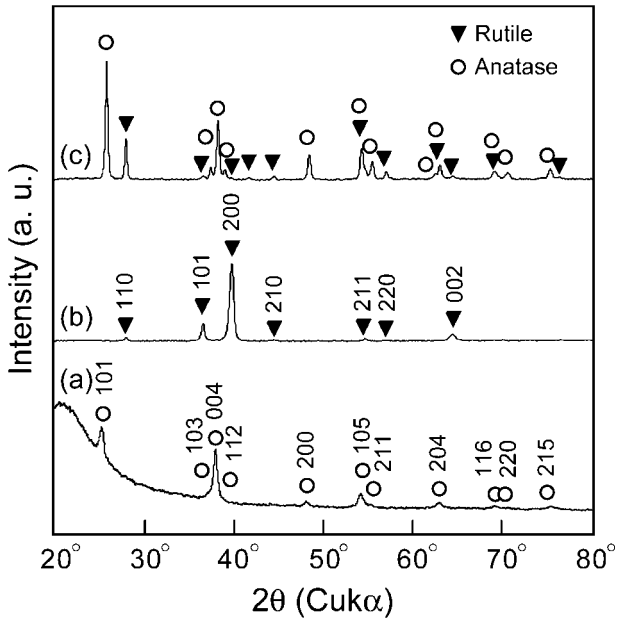

Fig. 1 X-ray patterns of TiO_2 films prepared at $T_{dep} = 723$ (a), 873 (b) and 1073 K (c).

grown at high T_{sub}. The (004) plane of anatase has a low atom-packing density[17] whereas the (101) is the lowest surface energy plane.[18] Then, the preferred orientation of anatase TiO_2 films might change from (004) to (101) with increasing T_{sub}. The (200) of rutile has a low atom-packing density and the (110) of rutile is the lowest surface energy plane.[19] Then, the preferred orientation of rutile TiO_2 films would change from (200) to (110) with increasing T_{sub}. These trends are well coincide with the experimental results shown in Fig. 1.

Figure 2 depicts the effects of T_{sub} and P_{tot} on the crystal phase of TiO_2 films. At $T_{sub} > 973$ K, the TiO_2 films were mixtures of anatase and rutile. Rutile TiO_2 films in a single phase were obtained at $T_{sub} = 873$ K and $P_{tot} = 0.6$ to 0.8 kPa. At T_{sub} between 723 and 873 K, the TiO_2 films became again mixtures of anatase and rutile. Anatase TiO_2 films in a single phase were obtained between 600 and 723 K. No films were formed at $T_{sub} < 600$ K.

Figure 3 demonstrates the effect of T_{sub} on the deposition rate (R_{dep}) in the Arrhenius format. The R_{dep} increased with increasing T_{sub} and then became almost constant or slightly decreased, showing a maximum R_{dep} (30 μm h^{-1}) at $T_{sub} =$ 973 K and $P_{tot} = 0.6$ kPa. The R_{dep} of the rutile TiO_2 films in a single phase was about 20 μm h^{-1}, which was almost the same as that reported by Krumdieck *et al.* ($R_{dep} = 20$ to 25 μm h^{-1}).[20] On the other hand, the R_{dep} of the anatase TiO_2 films in a single phase was about 1 μm h^{-1} that was higher than the value (0.4 μm h^{-1}) reported by Kim *et al.*[8]

Figure 4 depicts the surface and cross-sectional SEM image of TiO_2 films prepared at $P_{tot} = 0.8$ kPa and $T_{sub} =$ 723 to 1073 K. The anatase TiO_2 film obtained at 723 K showed a fine needle-like surface (Fig. 4(a)) with a dense cross-section (Fig. 4(b)). The grain size was about several 10 nm. The rutile TiO_2 film obtained at 873 K had a pebble-like surface about 200 nm in grain size (Fig. 4(c)) and well-developed columnar cross-section (Fig. 4(d)). A high mag-

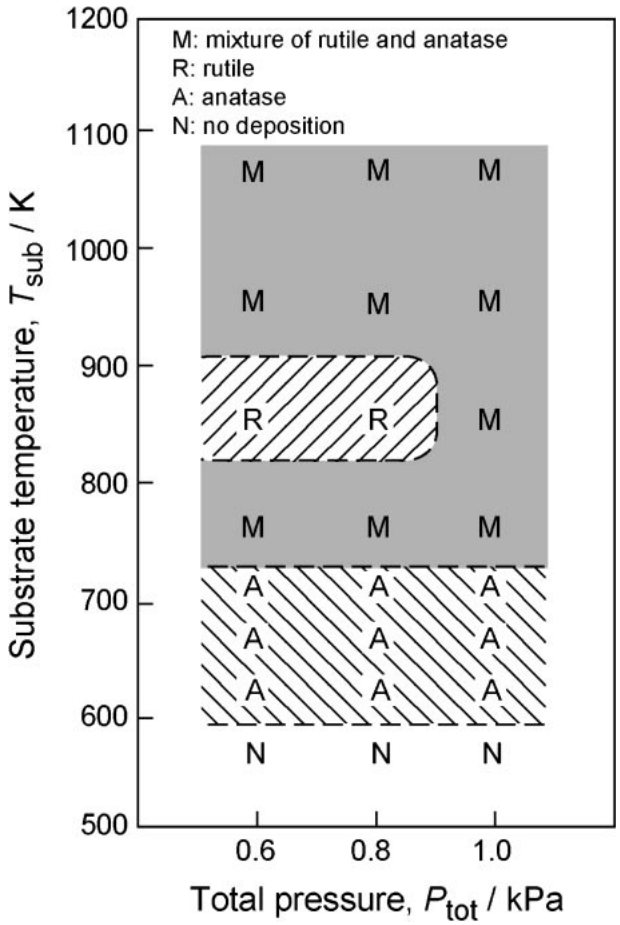

Fig. 2 Effects of P_{tot} and T_{sub} on the crystal phase of TiO_2 films. (A: Anatase, R: Rutile, M: Mixture of rutile and anatase, N: No-deposition)

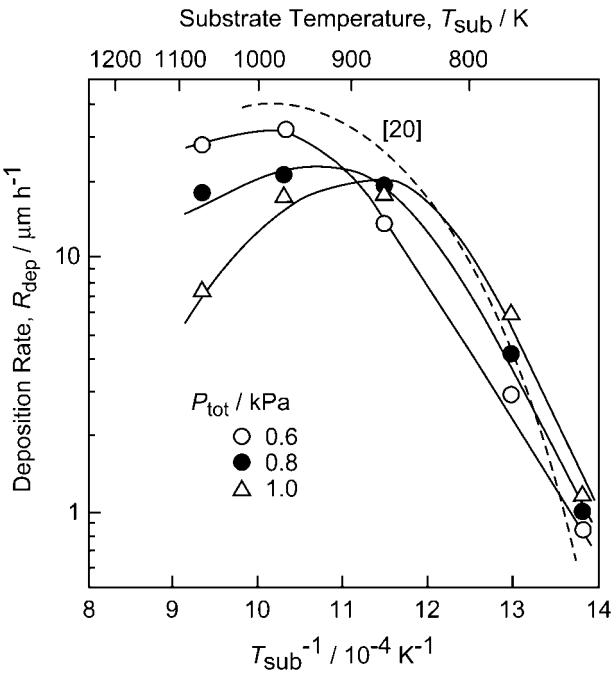

Fig. 3 Effect of T_{sub} on the deposition rate of TiO_2 films.

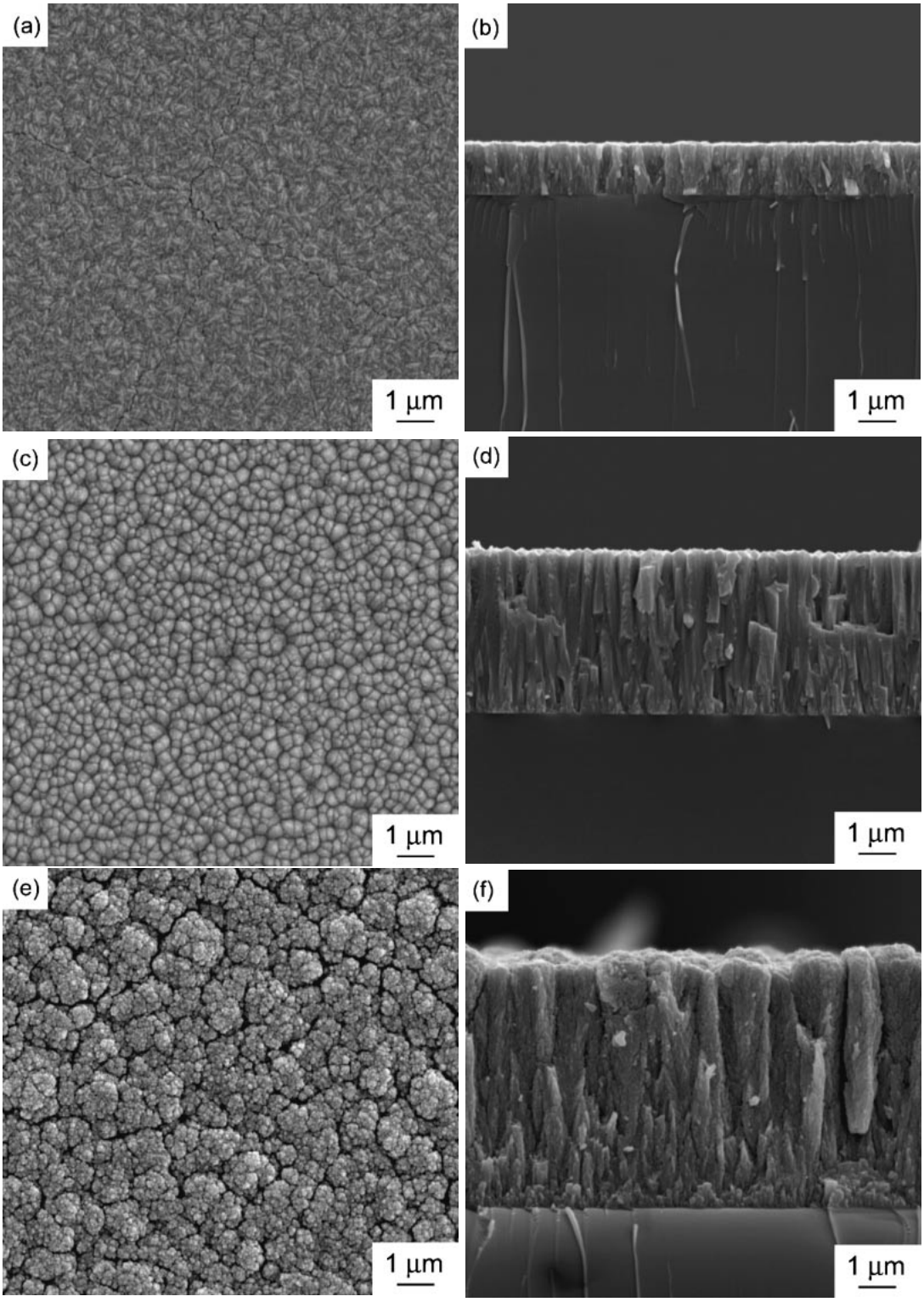

Fig. 4 Surface and cross-section of TiO_2 films prepared at $T_{dep} = 723$ (a), (b), 873 (c), (d) and 1073 (e), (f).

nification TEM image revealed many pores about 10 nm in diameter in the columnar grains. We have reported that a large amount of pores about 10 nm in diameter were contained in columnar grains of yttria stabilized zirconia (YSZ) films prepared by MOCVD and laser-assisted CVD.[21,22] The pores in nano-meter size tended to form in films prepared at a high deposition rate around several 10 to several 100 $\mu m\,h^{-1}$. The columnar structure would form due to a low mobility of atoms particularly to transverse direction. The lack of mobility might therefore result in the nano-sized porous micro-texture. The TiO_2 films prepared at 1073 K were mixture of anatase and rutile, and had a cauliflower-like surface about 100 nm in grain size with coarse columnar cross-section. Further study should be conducted to understand the formation mechanism of the nano-sized pores.

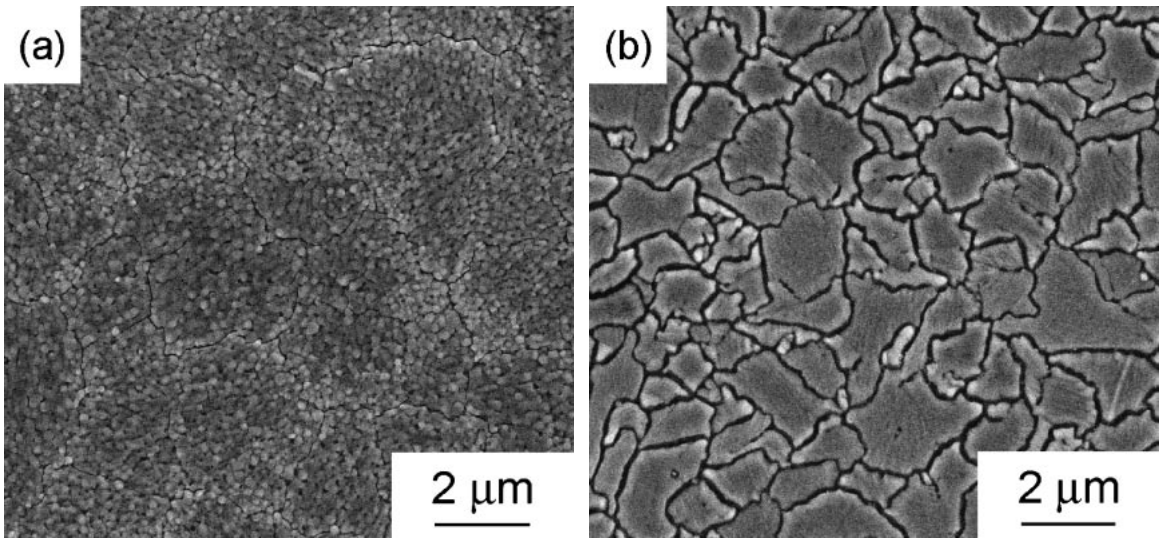

Fig. 5 Surface SEM images of anatase TiO_2 films after heat-treatment at 1323 (a) and 1373 K (b) in air for 10.8 ks.

Figure 5 shows the surface SEM images of the anatase TiO_2 film prepared at $P_{tot} = 0.8$ kPa and $T_{sub} = 723$ K after heat treated at 1323 to 1373 K. The TiO_2 film heat-treated at 1323 K had a granular microstructure about 100 nm in diameter, and cracks of several 10 nm in width (Fig. 5(a)). The anatase TiO_2 film heat-treated at 1373 K changed to a cracked dense plate-like surface about 1 to 2 μm in size, and the cracks were several 100 nm in width (Fig. 5(b)). The surface of anatase TiO_2 films heat-treated at below 1273 K showed almost no change.

Figure 6 shows TEM images of anatase TiO_2 films prepared at $P_{tot} = 0.8$ kPa and $T_{sub} = 723$ K after heat-treated at 1273 to 1373 K. As-deposited anatase TiO_2 film had a dense microstructure with granular grains about 5 nm in diameter (Fig. 6(a)). The anatase TiO_2 film heat-treated at less than 1273 K showed almost no grain growth, and many gaps about 2 nm in width were observed (Fig. 6(b)). The anatase TiO_2 film heat-treated at 1373 K showed a uniform microstructure and no granular grains (Fig. 6(c)).

Figure 7 shows XRD patterns of anatase TiO_2 film prepared at $P_{tot} = 0.8$ kPa and $T_{sub} = 723$ K after heat-treated at 1273 to 1373 K. As-deposited anatase TiO_2 film had a significant preferred orientation of (004) as shown in Fig. 1(a). With increasing the heat-treatment temperature, the (004) peak of anatase TiO_2 became sharper and the (101) peak intensity of anatase TiO_2 decreased. The anatase TiO_2 films heat-treated at less than 1273 K showed no phase transform to rutile (Fig. 7(a)–(c)). A rutile phase was detected after heat-treated at 1323 K (Fig. 7(d)). The transformation temperature (T_{AR}) of anatase TiO_2 films prepared by TTIP was around 1173 to 1273 K,[7] whereas that of anatase TiO_2 films prepared by TTB was 1073 to 1173 K.[13] The T_{AR} of anatase TiO_2 films prepared by $Ti(O\text{-}i\text{-}Pr)_2(dpm)_2$ in the present study was 1323 to 1373 K, much higher than those reported values. The anatase TiO_2 film heat-treated at 1373 K transformed to rutile with a strong (110) peak (Fig. 7(e)). Although the (110) peak is the highest in the XRD profile of rutile in International Centre for Diffraction Data,[23] other peaks were much less than those of the card, implying preferred (110) orientation. The (004) plane of anatase TiO_2 has a specific relationship with the (110) plane of rutile TiO_2 as depicted in Fig. 8.

Figure 9 shows the optical transmittance (O_t) of the anatase TiO_2 films prepared at $P_{tot} = 0.8$ kPa and $T_{sub} = 723$ K after heat-treatment at 1073 to 1373 K. The heat-treated anatase TiO_2 film showed an absorption edge at around a wave length (λ) of 300 nm. The O_t of the as-deposited anatase TiO_2 film was 60 to 80% at $\lambda > 400$ nm having the highest O_t of 78% at $\lambda = 550$ nm. The O_t increased with increasing heat-treatment temperature from 1073 to 1273 K. The anatase TiO_2 film heat-treated at 1173 K had the highest O_t over 90% at $\lambda = 450$ nm. However, the O_t of the films at $T_h = 1323$ to 1373 K slightly decreased in the visible light range, and the absorption edge shifted to higher λ. The optical bandgap (E_g) can be obtained from the relationship $(\alpha = \alpha_0(E - E_g)^2)$[24,25] between absorptance ($\alpha = 1/O_t$) and photon energy ($E = h\nu$). The E_g of the as-deposited was 3.27 eV, almost the same as that heat-treated at 1073 to 1173 K. The E_g of the anatase TiO_2 film heat-treated at 1273 K decreased to 3.17 eV, and further decreased to 3.05 eV heat-treated at 1323 K. It is known that optical bandgap of anatase and rutile TiO_2 are 3.25 eV and 3.0 to 3.05 eV,[24,26] respectively. Mardare *et al.* reported that the E_g of anatase TiO_2 film prepared by RF sputtering was 3.20 to 3.25 eV, and that of anatase-rutile mixture TiO_2 film was 3.11 to 3.15 eV.[25] Won *et al.* reported that the E_g of anatase TiO_2 film prepared by CVD was 3.5 eV. The anatase TiO_2 film heat-treated at 1073 K showed no phase transformation, and a slight transformation was identified by heat-treating at 1173 K resulting in the decrease of E_g to 3.2 eV.[7] In the present study, the T_{AR} of 1323 K was higher than those prepared by conventional sputtering and CVD.

Figure 10 shows the effect of heat-treatment temperature on the change of refractive index (n) of anatase TiO_2 film prepared at $P_{tot} = 0.8$ kPa and $T_{sub} = 723$ K. The heat-treatment temperature less than 1273 K caused no transformation, whereas that at more than 1323 K yielded in a mixture of anatase and rutile TiO_2, or rutile TiO_2 in a single phase. The n of as-deposited anatase TiO_2 film was 2.36 and increased with increasing heat-treatment temperature. The n

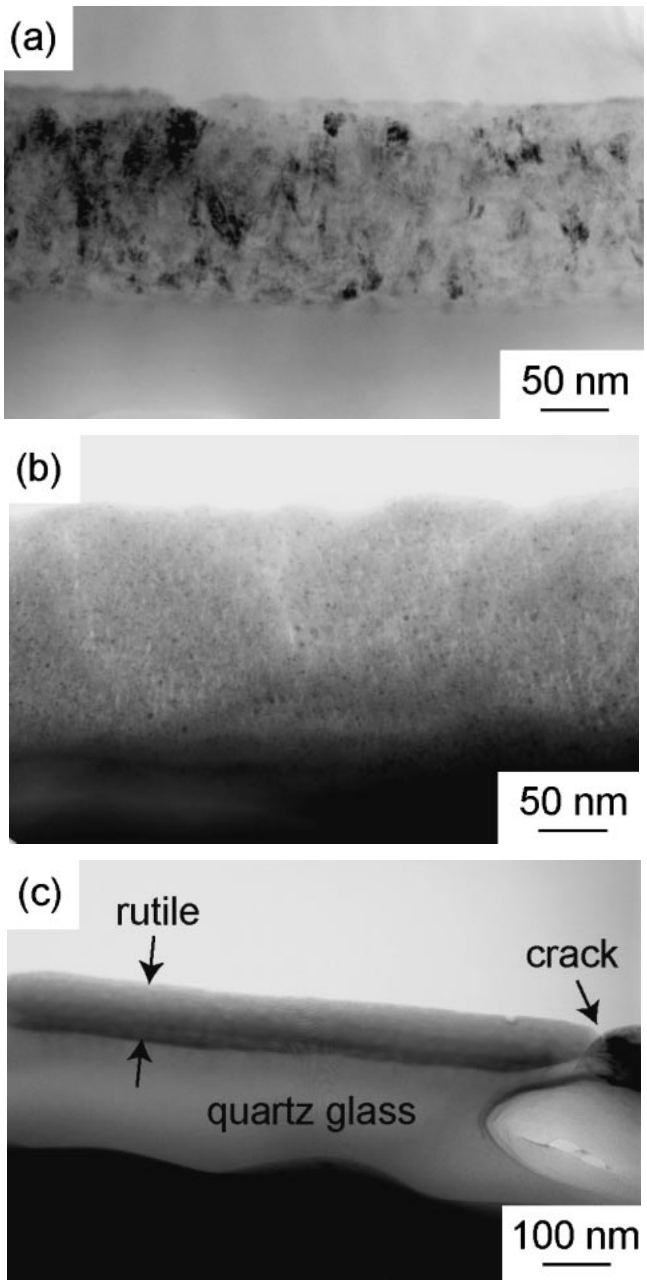

Fig. 6 Cross-sectional TEM images of anatase TiO_2 film (a) and that heat-treated at 1273 (b) and 1373 K (c) in air for 10.8 ks.

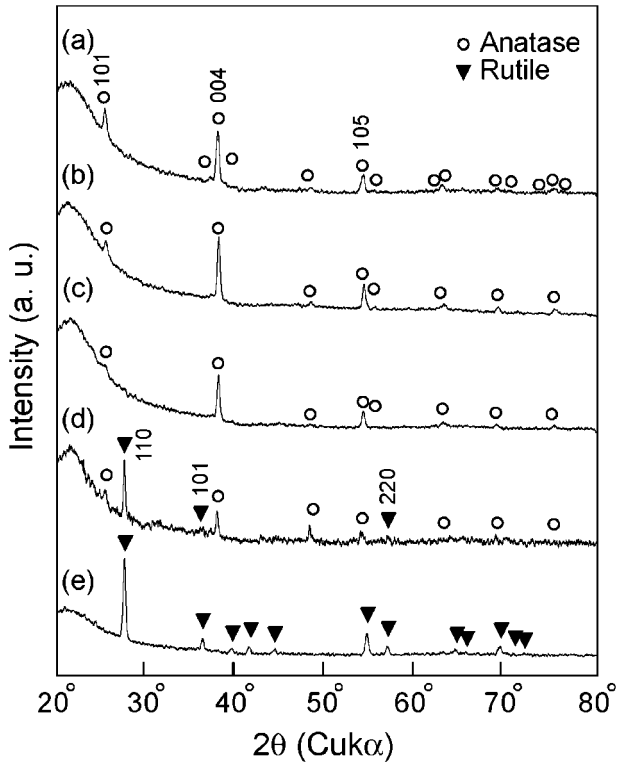

Fig. 7 X-ray patterns of anatase TiO_2 films after heat treatment at 1073 (a), 1173 (b), 1273 (c), 1323 (d) and 1373 K (e) in air for 10.8 ks.

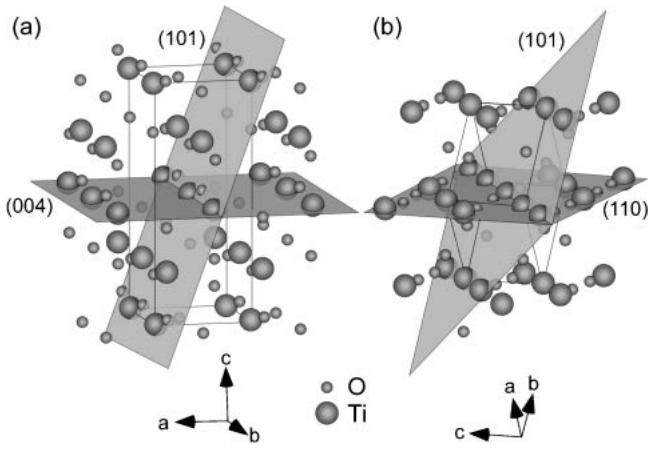

Fig. 8 Crystal structures of anatase (a) and rutile (b).

of the anatase TiO_2 film heat-treated at 1273 K increased to 2.58. This may be caused of the grain growth by the heat treatment. The crystallite size of as-deposited anatase TiO_2 film calculated from the Scherrer's equation[27] was 8 nm, and increased to 12 nm by heat-treating at 1273 K. The n of the mixture of anatase and rutile TiO_2 film heat-treated at 1373 K increased to 2.72. The n of anatase and rutile TiO_2 are known as 2.5 and 2.7,[28] respectively. Won *et al.* reported that the n of anatase TiO_2 film prepared by MOCVD was 2.0 at $\lambda = 623$ nm, and increased to 2.4 and 2.6 by heat-treating at 1073 and 1273 K,[7] respectively. They explained that the increase in n of anatase TiO_2 film heat-treated at 1073 K was resulted from the increase in density, whereas that at higher heat-treatment temperature would be caused of the transformation.[7] The n and T_{AR} in the present study were higher than those reported by Won *et al.*

Figure 11 shows the transformation temperature from anatase to rutile (T_{AR}) comparing to those in literatures. The anatase films prepared by sol-gel were reported to be transformed to rutile in between 873 and 1073 K.[29–31] The T_{AR} of the films prepared by sputtering was 1023 to 1173 K.[32,33] The anatase films prepared by CVD had higher T_{AR} than those prepared by sol-gel and sputtering, around 973 to 1273 K. Furthermore, the anatase film in the present study had the highest T_{AR} from 1323 to 1373 K. Kim *et al.* reported that the T_{AR} of anatase particles synthesized by CVD using TTIP was ranged between 1073 and 1173 K; where the higher carbon content the lower T_{AR}. However, the amount of carbon content was not determined.[15] In the present study, the carbon content in the anatase films prepared by using $Ti(O\text{-}i\text{-}Pr)_2(dpm)_2$ was about 3 mol%

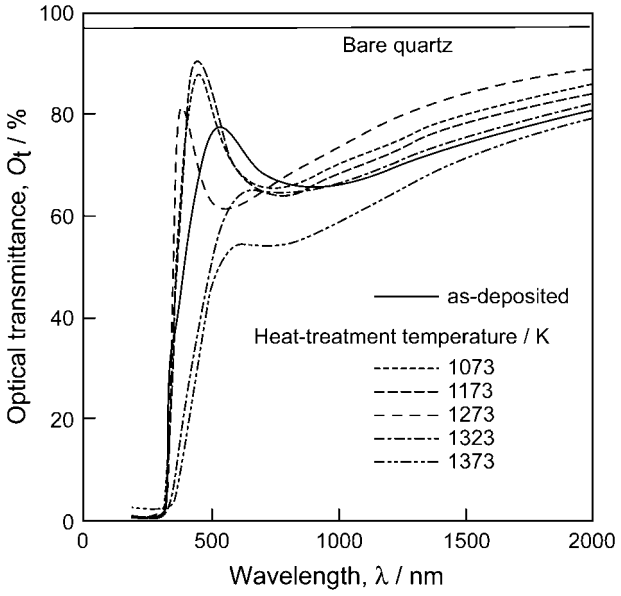

Fig. 9 Relationship between optical transmittance for heat-treated anatase TiO_2 films.

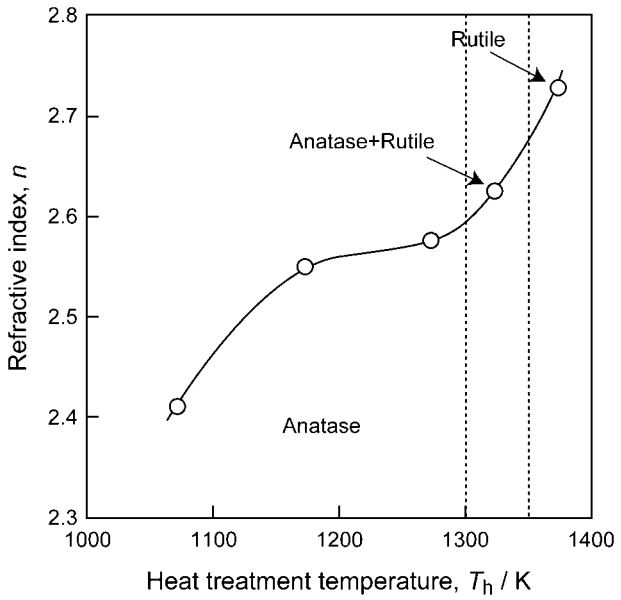

Fig. 10 Effect of heat treatment temperature on the refractive index of anatase TiO_2 film.

according to Auger electron spectroscopy. Although the precise determination of carbon content is commonly difficult for films, the amount of 3 mol% carbon in the anatase film is rather low comparing with other processes such as sol-gel. The low content reasons for the high T_{AR} in the present study would be associated with the high T_{AR} of the present anatase TiO_2 films. The photocatalytic property of the anatase TiO_2 films will be reported elsewhere.

4. Conclusions

Anatase and rutile TiO_2 films in a single phase were prepared by MOCVD using a $Ti(O\text{-}i\text{-}Pr)_2(dpm)_2$ precursor. The anatase TiO_2 film in a single phase was obtained at $T_{sub} < 723$ K and $P_{tot} = 0.6$ to 1.0 kPa, and the rutile TiO_2 film in a single phase was obtained at $T_{sub} = 873$ K and $P_{tot} = 0.6$ to 0.8 kPa. The morphology of TiO_2 films changed from a needle-like to cauliflower-like surface and dense to coarse columnar cross-section with increasing T_{sub}. The anatase film showed no transformation by heat-treating less than 1273 K, and then transformed to rutile TiO_2 by heat-treating at 1373 K. The transformation temperature of the anatase TiO_2 film was 1323 to 1373 K, the highest in the literatures. The transmittance and optical bandgap of anatase films showed almost no change by heat-treating less than at 1273 K, whereas the refractive index increased from 2.36 to 2.58. The refractive index of the TiO_2 films increased from 2.58 to 2.72 with increasing heat-treatment temperature from 1273 to 1373 K, due to the transformation.

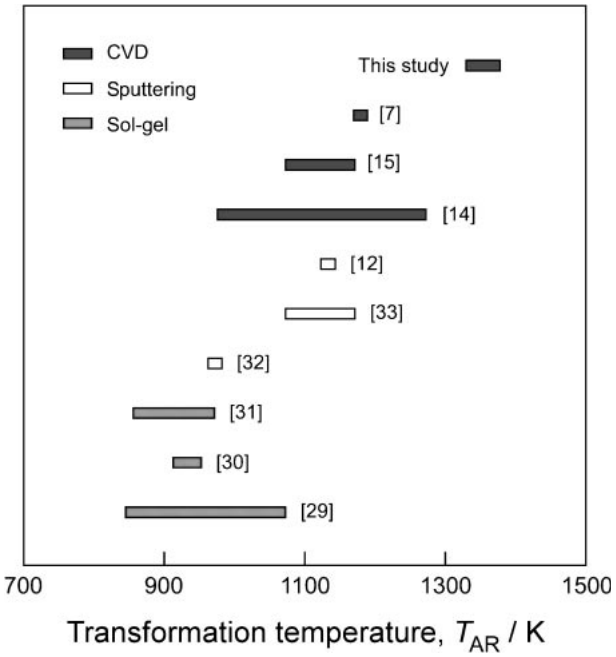

Fig. 11 Transformation temperature of TiO_2 from anatase to rutile.

Acknowledgement

This research was partially supported by the Global COE Materials Integration Program, Tohoku University and the Japan Society for the Promotion of Science (JSPS), Asian CORE program "Interdisciplinary Science of Nanometers."

REFERENCES

1) Y. H. Zhang, C. K. Chan, J. F. Porter and W. Guo: J. Mater. Res. **13** (1998) 2602–2609.
2) A. L. Linsebigler, G. Q. Lu and J. T. Yates: Chem. Rev. **95** (1995) 735–758.
3) K. N. P. Kumar, K. Keizer and A. J. Burggraaf: J. Mater. Sci. Lett. **13** (1994) 59–61.
4) D. J. Kim, S. H. Hahn, S. H. Oh and E. J. Kim: Mater. Lett. **57** (2002) 355–360.
5) D. H. Kuo and K. H. Tzeng: Thin Solid Films **420–421** (2002) 497–502.
6) D. Mergel, D. Buschendorf, S. Eggert, R. Grammes and B. Samset: Thin Solid Films **371** (2000) 218–224.
7) D. J. Won, C. H. Wang, H. K. Jang and D. J. Choi: Appl. Phys. A **73** (2001) 595–600.

8) B. Kim, D. Byun, J. K. Lee and D. Park: Jpn. J. Appl. Phys. **41** (2002) 222–226.
9) W. Li, C. Ni, H. Lin, C. P. Huang and S. Ismat Shah: J. Appl. Phys. **96** (2004) 6663–6668.
10) X. Ding, L. Liu, X. Ma, Z. Qi and Y. He: J. Mater. Sci. Lett. **13** (1994) 462–464.
11) C. Suresh, V. Biju, P. Mukundan and K. G. K. Warrier: Polyhedron **17** (1998) 3131–3135.
12) D. Wicaksana, A. Kobayashi and A. Kinbara: J. Vacuum Sci. Tech. A **10** (1992) 1479–1482.
13) Y. Sun, T. Egawa, L. Zhang and X. Yao: Jpn. J. Appl. Phys. Part 2-Lett. **41** (2002) L945–L948.
14) Y. J. Sun, A. Z. Li, M. Qi, L. Y. Zhang and X. Yao: Mater. Sci. Eng. B **86** (2001) 185–188.
15) C. S. Kim, K. Nakaso, B. Xia, K. Okuyama and M. Shimada: Aerosol Sci. Tech. **39** (2005) 104–112.
16) R. Tu, T. Kimura and T. Goto: Mater. Trans. **43** (2002) 2354–2356.
17) M. Lazzeri, A. Vittadini and A. Selloni: Phys. Rev. B **63** (2001) 155409-1–9.
18) U. Diebold, N. Ruzycki, G. S. Herman and A. Selloni: Catalysis Today **85** (2003) 93–100.
19) M. Ramamoorthy, D. Vanderbilt and R. D. King-Smith: Phys. Rev. B **49** (1994) 16721–16727.
20) S. Krumdieck and R. Raj: Surf. Coat. Tech. **141** (2001) 7–14.
21) T. Kimura and T. Goto: Surf. Coat. Tech. **198** (2005) 129–132.
22) T. Kimura, R. Tu and T. Goto: J. Japan Inst. Metals **69** (2005) 12–16.
23) *International Centre for Diffraction Data*, No. 21-1276, Joint Comittee on Powder Diffraction Standards.
24) H. Tang, K. Prasad, R. Sanjinès, P. E. Schmid and F. Lévy: J. Appl. Phys. **75** (1994) 2042–2047.
25) D. Mardare, M. Tasca, M. Delibas and G. I. Rusu: Appl. Surf. Sci. **156** (2000) 200–206.
26) N. Daude, C. Gout and C. Jouanin: Phys. Rev. B **15** (1977) 3229–3235.
27) L. J. Meng and M. P. Dos Santos: Thin Solid Films **226** (1993) 22–29.
28) G. S. Brady and H. R. Clauser: *Mater. Handbook*, 13th ed., McGrawHill, New York, 1991.
29) P. J. Huang, H. Chang, C. T. Yeh and C. W. Tsai: Thermochimica Acta **297** (1997) 85–92.
30) R. Arroyo, G. Córdoba, J. Padilla and V. H. Lara: Mater. Lett. **54** (2002) 397–402.
31) H. Zhang and J. F. Banfield: J. Phys. Chem. B **104** (2000) 3481–3487.
32) G. He, Q. Fang, L. Zhu, M. Liu and L. Zhang: Chem. Phys. Lett. **395** (2004) 259–263.
33) E. San Andrés, M. Toledano-Luque, A. del Prado, M. A. Navacerrada, I. Mártil, G. González-Díaz, W. Bohne, J. Röhrich and E. Strub: J. Vac. Sci. Technol. A **23**(6) (2005) 1523–1530.